

Electronic structure of the minimum-diameter TI, Pb and Bi quantum wire superlattices

This article has been downloaded from IOPscience. Please scroll down to see the full text article.

1993 J. Phys.: Condens. Matter 5 1081

(<http://iopscience.iop.org/0953-8984/5/8/009>)

View [the table of contents for this issue](#), or go to the [journal homepage](#) for more

Download details:

IP Address: 171.66.16.159

The article was downloaded on 12/05/2010 at 12:57

Please note that [terms and conditions apply](#).

Electronic structure of the minimum-diameter Tl, Pb and Bi quantum wire superlattices

S Romanov

A Ioffe Physical Technical Institute, Polytechnicheskaya Ulitsa 26, St Petersburg 194021, Russia

Received 13 April 1992, in final form 19 October 1992

Abstract. On the basis of the analysis of the optical absorption spectra and conductivity data the model of the electronic structure of the regular three-dimensional arrays of minimum-diameter (0.6 nm) quantum wires of Tl, Pb and Bi has been proposed. It is characterized by a dielectric type of energy spectrum, an atomic-like energy band structure near the gap, anisotropy of this spectrum and localization of the electronic states near the gap.

1. Introduction

In recent years there has been a revival of interest in minimum-size particles, clusters and wires consisting of a small number of atoms. This is because of the progress in the physics of nanostructures, i.e. successful technology development and new physical properties [1]. The electronic structures of bulk materials and isolated atoms are known exactly, but the electronic structure of nanoparticles with numerous atoms is of special interest and is not known exactly.

Experimental study of the interface between the band structure and atomic levels is possible only with a macroarray of identical particles. At present, only two types of array of nanoparticles may have this feature: the metal–organic cluster materials [2] and clusters incorporated in crystalline porous matrices [3]. Unfortunately, the electronic structure of metal clusters in an organic environment is strongly affected by the chemical bond with a ligand. In this sense, clusters embedded in a dielectric framework keep their individuality since the matrix–inclusion interaction is weaker than the binding energy between atoms in the cluster. That is why experimental data on the electronic structure of matrix inclusions reflect mainly the properties of the nanoparticles themselves.

Earlier we have reported that the electronic spectra of metal and semiconductor nanoparticulates in zeolite cavities are similar to the spectra of dielectric materials owing to the strong electron confinement [5]. The aim of this work is to select some general features of the electronic spectra of crystalline arrays of minimum-diameter Tl, Pb and Bi wires (denoted below as M–Tl, M–Pb and M–Bi, respectively).

2. Samples

In this work the method of cluster design consisting in impregnating a porous dielectric crystalline matrix with molten metal under a high pressure was applied

[3]. The matrix used is the natural zeolite mordenite (M); the structure of the crystalline framework possesses a system of parallel channels inside it [4]. The inner channel diameter is 0.67 nm and the free channel volume is 19% of the whole crystal volume. All the channels are arranged along the c axis of the crystal with a distance of 1.35 nm between the centres of nearest neighbours (figure 1).

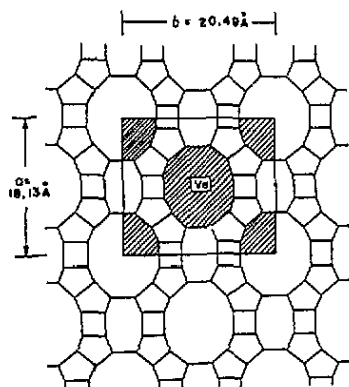


Figure 1. View of the M structure across the channel direction.

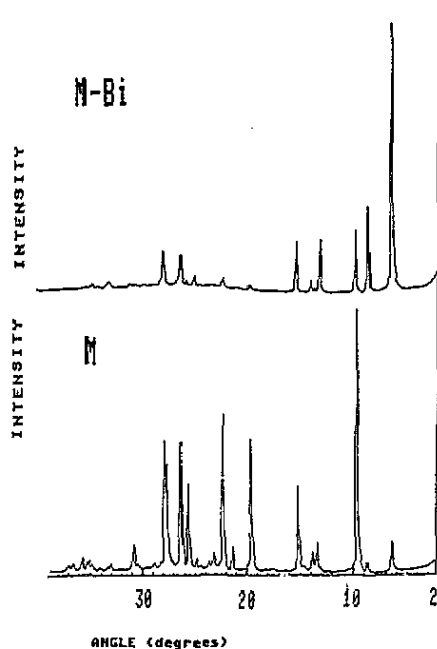


Figure 2. X-ray diffraction patterns of M before and after Bi is added (line Co $K\alpha$; $\lambda = 0.17902$ nm).

The composition per unit cell of the natural M crystal used was $\text{Na}_{4.16}\text{Ca}_{2.12}\text{K}_{0.096}\text{Al}_{8.56}\text{Si}_{39.5}\text{O}_{96}\cdot 28\text{H}_2\text{O}$. With the aim of channel widening, the cations Na^+ , K^+ and Ca^{2+} were replaced by H^+ . Finally, after ion exchange, dehydration and, for example, a Bi melt treatment the composition was $\text{Na}_{0.51}\text{Ca}_{1.81}\text{Al}_{7.14}\text{Si}_{39.5}\text{O}_{132}\text{Bi}_{12.59}$. Thus the sample contains nearly six Bi atoms in one channel per M unit cell length $c = 0.752$ nm (the corresponding concentration

of Bi atoms is $4.5 \times 10^{21} \text{ cm}^{-3}$). Clear proof of the wire lattice formation was obtained from a comparative analysis of the M and M-Bi diffractograms (figure 2); the M-Bi picture exhibits crystalline ordering like the M crystal, and moreover its most significant feature is the sharp enhancement of the reflection at 6.5° corresponding to the minimum interchannel distance of 1.37 nm. As for the M-Tl and M-Pb samples, they contain nearly 3.5 metal atoms per channel within a unit cell. The homogeneity of the metal distribution in the matrix was examined over $1 \mu\text{m}$ length, but it is not sufficient to estimate the real length of interrupted wires. Taking into account the inner channel diameter and the regular channel arrangement, it may be found that crystalline macroscopic arrays of extremely thin wires (one atom per cross section in the case of M-Tl and M-Pb, and two atoms in the case of M-Bi) were successfully prepared using M.

Some suggestions on which to base the model of the bonding structure of Bi wire are now considered. The outermost electronic shell configuration of the Bi atom is $6s^26p^3$. Because of the 9 eV difference between the s and p orbitals, the sp hybridization scarcely takes part in the chemical bond formation, and deep s electrons do not contribute to the bond between Bi atoms, i.e. the typical Bi valence is 3. Under this condition the bonding structure of the Bi wire in the M channel looks like a double zigzag chain of threefold-coordinated atoms (figure 3). This chain is characterized by a 0.3 nm bond length and 90° bond angle (0.31 nm and 90° for bulk Bi). The period of this chain is nearly 0.42 nm; therefore the commensurability with the matrix period is achieved at three to four periods of the Bi chain. In the cases of M-Tl and M-Pb the structure of the metal chains is scarcely predictable because of the strong mixing of s and p states in the chemical bond between the metal atoms.

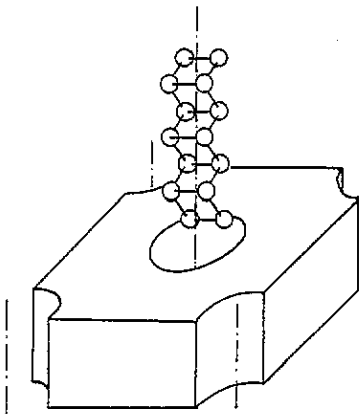


Figure 3. Schematic view of the proposed structure of the Bi chain in the M channel.

3. Experimental techniques

The experimental data were obtained by means of optical absorption spectroscopy accompanied by conductivity measurements. Both single crystals and powders were used because of the small size of the M single crystals; a typical crystal size is $0.05 \text{ mm} \times 0.01 \text{ mm} \times 0.1 \text{ mm}$ and the size of the powder particles is about 0.001 mm. The optical density spectra $D(h\nu)$ of the single crystals were measured in the range

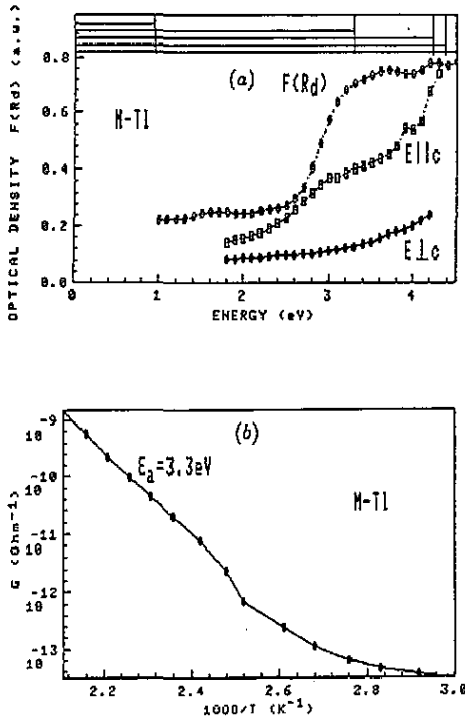


Figure 4. (a) Polarized absorption spectra of the M-Tl single crystal (absorption is given in units of optical density) together with the $F(R_d)$ spectrum (a.u., arbitrary units). In the upper part the energies of the transitions from the ground state to the excited states of the Tl atom are shown for reference. (b) Temperature dependence of the conductivity of a powdered sample.

from 1 to 4 eV using a microspectrophotometer with the light polarized along $E||c$ and across the $E \perp c$ wire direction from a square 0.01 mm \times 0.01 mm with a sample thickness of a few microns. The diffuse reflection spectra $R_d(h\nu)$ of powders were measured in the range from 1 to 5.5 eV; then the function $F(R_d)$, which correlates with the absorption spectra, was calculated using a standard procedure [6]. The electrical methods used were measuring the current-voltage characteristics (by a four-probe method) and the temperature dependences of the DC conductivity, AC conductivity and AC photoconductivity at 10 GHz.

4. Results and discussion

The large number of metal atoms in the wire, their close displacement and interwire interaction lead to the formation of extended energy bands of the metal subsystem of the sample. As was shown earlier [7], the conduction and valence bands of the 'guest' material are located near the centre of the matrix gap (M gap $E_g = 10$ eV); therefore the observed optical absorption in the range from 1 to 5 eV may be attributed to zeolite inclusions.

The absorption spectra of the investigated samples (figures 4-6) yield clear evidence of the 'guest' energy band formation. In all cases an increase in the absorption which may be ascribed to the absorption edge was observed. The $E_{g, \text{opt}}$ -values of 2.9 eV, 1.56 eV and 1.1 eV for M-Tl, M-Pb and M-Bi, respectively, were determined using diffuse reflection spectra by means of Fochs' [8] criterion. It is also easy to see that the $E_{g, \text{opt}}$ -values obtained correspond well to the activation energies E_a of conductivity at high temperatures, 3.3 eV, 1.36 eV and 1.23 eV (these

are average values for a set of samples) for M-Tl, M-Pb and M-Bi, respectively. Linearity of the current-voltage curves in a wide range of electrical fields from 0.1 to 10000 V cm⁻¹ confirms the band character of the conductivity.

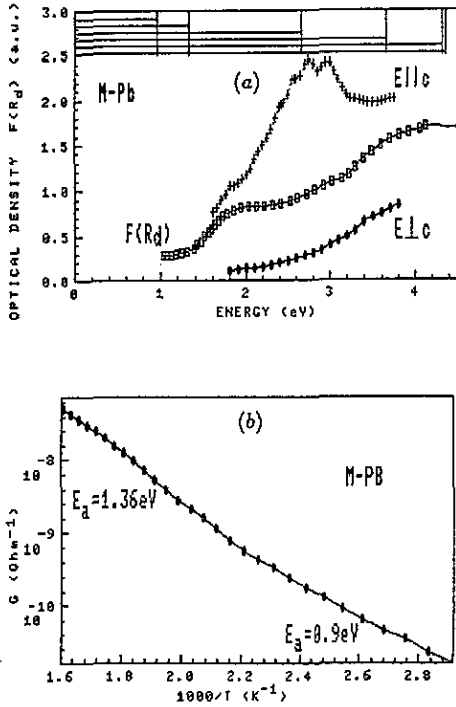


Figure 5. (a) Polarized absorption spectra of the M-Pb single crystal together with the absorption $F(R_d)$ (a.u., arbitrary units). In the upper part the transitions from the ground state to the excited states of the Pb atom are indicated. (b) Temperature dependence of conductivity.

The approximate energy scale of the observed gap is about 1 eV. This value is close to that obtained from energy level splitting in the case of a quantum wire [9]:

$$E = \hbar^2(\lambda_s^{|m|})/2m_{\perp}r^2 + \hbar^2k^2/2m_{\parallel}$$

for a radius $r = 0.33$ nm and $m_{\perp}/m_{\parallel} = 10$, where m_{\parallel} and m_{\perp} are the effective electron masses in the directions along and across the wire. $m_{\parallel} = m_0$ is the mass of the free electron. This ratio of effective masses roughly corresponds to the observed anisotropy rate of absorption spectra. $\lambda_s^{|m|}$ is the s root of the Bessel function; $\lambda_s^{|m+1|} - \lambda_s^{|m|} = 1.2$; $m = 0, \pm 1, \pm 2, \dots$ is the magnetic quantum number.

It was first found in [5] that the positions of the peaks and shoulders of the absorption spectrum of zeolite incorporating eight-atom indium clusters correlate with the energies of the transitions from the ground state to the first, second, etc, excited states of an isolated indium atom, i.e. this spectrum may be considered as an atom-like spectrum. Apparently, the observed absorption may be assigned to the transitions in the subbands of the quantized electronic structure of the cluster material and so it reflects the energy distribution of the density of states of this material.

Figure 4 shows the absorption spectra of M-Tl. Peaks at 3.0 and 3.9 eV and a shoulder at 3.3 eV in both the $D_{\parallel}(\hbar\omega)$ and the $F(R_d)$ spectra are seen. Some correlation between these spectra and the transitions from the ground state to the excited states of the isolated Tl atom at 0.966, 3.28, 4.23, 4.36, 4.48 and 4.49 eV

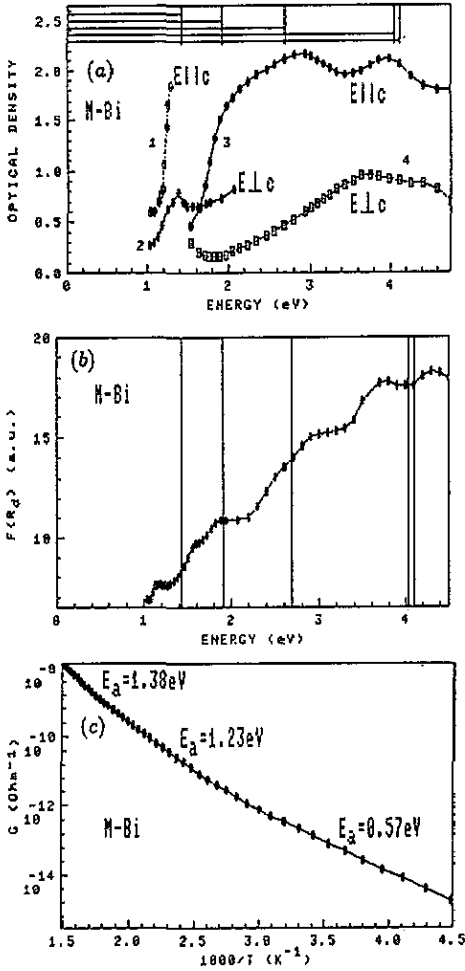


Figure 6. (a) Polarized absorption spectra of the M-Bi single crystal (curves 3 and 4), together with those for a thicker crystal (curves 1 and 2). In the upper part the transitions from the ground state to the excited states of the Bi atom are shown. (b) Absorption $F(R_d)$ spectrum for a powdered sample (a.u., arbitrary units). (c) Temperature dependence of conductivity.

(these transitions are indicated in the upper part of figure 4(a); the designation of these transitions in spectral terms is given elsewhere [10]) may be found. It needs to take into account that the first transition of the Tl atom is forbidden as a transition between states with the same symmetry and the absence of absorption near 1 eV in the case of M-Tl may be the result of this. On increase in the Tl content the intensity of the low-energy part of the spectrum increases (band centred at 1.7 eV and shoulder at 2.3 eV in $F(R_d)$). Correspondingly the colour of the M-Tl crystal changes from yellow to dark brown.

In the $D_{||}(\hbar\omega)$ spectrum for M-Pb the edge at 1.36 eV, a band near 1.8 eV, a four-component split maximum (2.4, 2.5, 2.7 and 2.9 eV) and singularities at 3.3 and 3.7 eV are observed (figure 5). This spectrum is confirmed by the $F(R_d)$ spectrum. The shape of this spectrum is in good agreement with the transition energies of the Pb atom of 0.969, 1.32 (these two transitions are forbidden), 2.66, 3.65, 4.33 and 4.37 eV indicated in figure 5. Also the absence of M-Pb absorption near 1 eV is related to the fact that the corresponding transitions of the Pb atom are forbidden.

The M-Bi crystal exhibits a $D_{||}(\hbar\omega)$ spectrum similar to that considered above. The spectral features are an edge at 1.1 eV, a shoulder at 1.9 eV, and maxima at

2.9 and 4 eV. Also, in the $D_{\perp}(\hbar\omega)$ spectrum (curve 2) a maximum at 1.4 eV with a shoulder at 1.2 eV is observed. With respect to the Bi atom the transitions at 1.42, 1.91, 2.68, 4.04 and 4.11 eV are known. Note that all these transitions are allowed and all contribute to the spectra of M–Bi.

It would be strange if the described correlations appear accidentally. On the one hand, under the quantum confinement of the electrons in the wire the extrema of the density of states are the result of the splitting of the ‘bulk’ energy bands into a set of narrow subbands [10]. On the other hand, if the free atoms become associated at the cluster, their energy levels spread into energy bands. Apparently, the energy spectrum of an array of extremely thin wires in the case of metal embedded in M has a subband structure genetically related to the atomic levels. Thus the observed shape of the absorption spectra and the sets of different activation energies of conductivity (0.9 and 1.36 eV for M–Pb; 1.23 and 1.38 eV for M–Bi) may be explained well by this model. However, it should be borne in mind that, specifically for one-dimensional (1D) systems, the two-band structure of the M–Bi absorption spectrum correlates with the idea of density-of-states maxima at the end and in the centre of the 1D Brillouin zone; moreover the interband distance of 1.1 eV is determined by the width of this zone.

Another feature of the spectra considered is the correlation of several spectral singularities with the transitions between the first and the next excited levels of an isolated atom: the shoulder at 2.3 eV in the M–Tl spectrum, the band at 1.8 eV in the M–Pb spectrum, and the shoulder at 1.2 eV in the M–Bi spectrum. The non-zero electron density in the first subband may be the result of the excitation due to the excess energy provided by the high-pressure impregnation of the matrix by the molten metal (the average energy of this excitation may be up to 0.3 eV/atom). According to [11], the interaction between the ‘guest’ atoms and the internal matrix surface occurs by means of excimer-like states at the interface between the matrix and the wire, and it leads to the partial occupancy of the excited levels. It was also found that an increase in the matrix loading, i.e. in the metal content in the matrix, leads to enhancement of the low-energy absorption. Apparently, this happens because of the more intensive interaction of the wire atoms with the matrix surface and a corresponding increase in the occupancy of the excited states. The channel loading may be controlled by the rate of cation exchange [12], but this property was not used intentionally in this work.

The rates of absorption anisotropy observed from figures 4–6 are 5 for M–Tl, 8 for M–Bi and 10 for M–Pb; moreover the shape of $D_{\perp}(\hbar\omega)$ differs significantly from that of $D_{\parallel}(\hbar\omega)$. As was shown in the case of Se wires embedded in M, two contributions may be seen in their $D_{\perp}(\hbar\omega)$ spectrum: transitions across one wire, and transitions across the array of wires [13–15]. The edge of $D_{\perp}(\hbar\omega)$ is formed by tunnel transitions between the states at the adjacent wires. It is characterized by an exponential increase in D_{\perp}/D_{\parallel} with increasing $\hbar\omega$ in the energy region of the D_{\parallel} edge. In this region the optical transitions across one wire are forbidden because of the selection rules; then, as soon as they become allowed, the maximum D_{\perp} is observed. However, in real samples the role of the selection rules is decreased because of the reduction in the wire symmetry due to the defects in the wires and the wire–matrix and interwire interactions.

Such an approach is appropriate for Tl- and Pb-based crystals, but it is unacceptable for M–Bi because of the absorption band at 1.4 eV in $D_{\perp}(\hbar\omega)$. Since the amount of Bi in M–Bi is higher than the amounts of Tl and Pb in M–Tl and M–Pb, respectively, its interwire interaction is also higher, and an extended energy band

across the array is formed. The observation of radio-frequency photoconductivity of M-Bi is also consistent with the idea of 3D energy band formation. This spectrum has a narrow peak (half-width, 0.047 eV) centred at 1.475 eV. The position and width of this peak correspond rather well to the absorption band in the $D_{\perp}(\hbar\omega)$ spectrum.

The observed anisotropy $\rho_{\perp}/\rho_{\parallel}$ of the resistivity for M-Bi is 30. It does not reflect the difference between the conductivities along and across the wire array, since any defect in the wire interrupts the current line. If the penetrability of the defect energy barrier is similar to that for a jump to the next wire, then the approximate length L of uninterrupted wire is near 20 nm. Thus, an $L/2r$ ratio of 330 characterizes the 1D electronic structure of the material considered.

The intrinsic property of 1D systems is the localization of their electronic states near the gap. Some evidence of localization was obtained by analysis of the M-Bi crystal absorption edge shape. It is possible to see several regions in the absorption spectra: an exponential Urbach-type tail (characteristic of transitions in disordered systems) and power-law parts with the dependence $D(\hbar\omega) \sim (\hbar\omega - E_g)^n$ with $n = 3$ and 0.75 for D_{\parallel} and $n = 2.5$ for D_{\perp} (figure 7). High exponent values are known for forbidden transitions and typical of those between localized states in disordered systems [14] (for direct allowed transitions, $n = 0.5$). The conductivity data are complementary to the optical data. In particular, for M-Bi the frequency-dependent hopping-type conductivity shunts the direct conductivity beginning at 10 Hz ($T = 300$ K), and up to 10 GHz the correlation $\rho \sim \hbar\omega^{-0.6}$ holds (at 10 GHz, $\rho = 1 \Omega \text{ cm}$) (figure 8). Moreover, the activation energy decreases with increase in frequency typically for highly localized 1D systems (figure 9) [16].

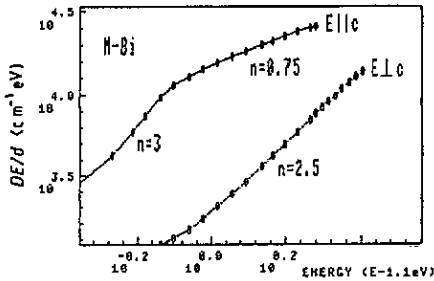


Figure 7. Absorption edges of the M-Bi crystal for light polarized along and across the wire direction.

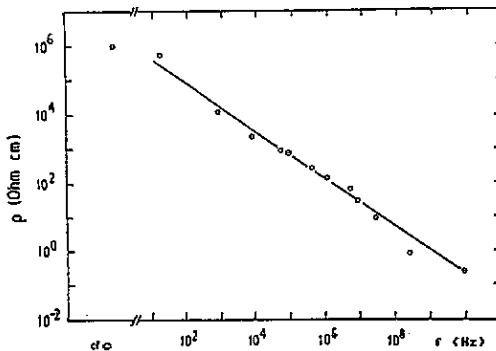


Figure 8. Frequency dependence of the conductivity of M-Bi powder.

The important problem is the alignment of the 'host' and 'guest' components of the energy structure of a composite system. In general, some mutually exclusive cases are possible:

- (i) a weak van der Waals type of coupling between the incorporated atoms of the metal themselves and between these atoms and the inner matrix surface, i.e. the absence of the 'guest' energy band;
- (ii) chemical coupling between atoms of metal and the M framework, i.e. formation of the impurity band in the matrix energy gap;
- (iii) a chemical bond (metallic or covalent—it is not clear at present) between the 'guest' atoms, i.e. the formation of their own energy structure regardless of the matrix structure.

To make the correct choice it is necessary to take into account

- (1) the existence of the absorption band near 5 eV in the spectrum of the sample before and after impregnation of the matrix by the metal (this band is assigned to absorption by oxygen defects of the M framework),
- (2) the need for the individual energy structure of the incorporated atoms to be kept and
- (3) the evidence of extended energy bands of the metal component of the composite solids investigated.

Model (i) does not agree with point (3), and model (iii) does not answer points (1) and (2); therefore, in my opinion model (ii) is preferable, although some kind of superposition of the models may be present.

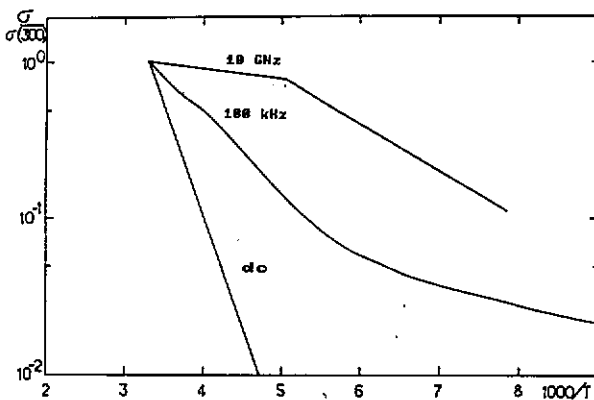


Figure 9. Temperature dependences of the conductivity of an M-Bi powdered sample at different frequencies.

5. Summary

The electronic structure of crystalline arrays of extremely thin wires of metals is determined by quantum confinement. By considering the energy spectrum of metal wires in zeolite channels to be that of a dielectric, the limit defined by the energy

difference between the ground and excited state of isolated atoms of this metal is achieved. The energy bands of the quantum metal wires are split into subbands, the energy positions of which correspond to the energy structure of the outermost electronic shell of the excited atom. As a rule a quasi-1D type of electronic structure is formed, but with increased metal content the 3D type is possible.

Acknowledgments

The author wishes to thank V Bogomolov for suggesting the system investigated and Y Alekseev, S Kholodkevich and V Petranovsky for useful discussions.

References

- [1] Stucky G D and MacDaugall J E 1990 *Science* **247** 669
- [2] Steingerwald L D *et al* 1986 *J. Am. Chem. Soc.* **110** 3046
- [3] Bogomolov V N 1978 *Sov. Phys.-Usp.* **21** 77
- [4] Breck D W 1984 *Zeolite Molecular Sieves* (Malabar, FL: Krieger)
- [5] Alekseev Y, Bogomolov V, Kholodkevich S, Petranovsky V, Romanov S and Zhukova T 1986 *Izv. Akad. Nauk. SSSR, Ser. Fiz.* **50** 418 (in Russian)
Bogomolov V, Kholodkevich S, Romanov S and Agroskin L 1983 *Solid State Commun.* **47** 181
- [6] Kubelka P and Munk F 1931 *Z. Tech. Phys.* **12** 593
- [7] Gagarin S, Teterin Y, Komarov V, Urbanovich I and Gintovt T 1984 *Dokl. Akad. Nauk. SSSR* **274** 1087 (in Russian)
- [8] Fochs P D 1956 *Proc. Phys. Soc. B* **60** 70
- [9] Tavger B, Bloch M and Fishman E 1972 *Fiz. Metall. Metalloved.* **33** 1137 (in Russian)
- [10] Radcig A and Smirnov B 1980 *Handbook of Atomic and Molecular Physics* (Moscow: Atomizdat)
- [11] Bogomolov V N 1992 *Zh. Tekh. Fiz.* **62** 152 (in Russian)
- [12] Nozue Y, Kodaira T, Terasaki O, Yamazaki K, Goto T, Watanabe D and Thomas J M 1990 *J. Phys.: Condens. Matter* **2** 5209
- [13] Bogomolov V, Poborchii V, Romanov S and Shagin S 1985 *J. Phys. C: Solid State Phys.* **18** L313
- [14] Afonin V and Pogorelsky Y 1981 *Sov. Phys.-Solid State* **23** 3164
- [15] Mott N and Davis E 1971 *Electronic Processes in Non-Crystalline Materials* (Oxford: Clarendon)
- [16] Zettle A, Jackson C M and Garner G 1982 *Phys. Rev. B* **26** 5773